Improved Particle Confinement with Resonant Magnetic Perturbations in DIII-D Tokamak H-Mode Plasmas

N. C. Logan[1,*] Q. Hu[2] C. Paz-Soldan[3,†] R. Nazikian[2,‡] T. Rhodes[4] T. Wilks[5] S. Munaretto[3,§]
A. Bortolon[2] F. Laggner[2] F. Scotti[1] R. Hong[4] and H. Wang[3]

[1]*Lawrence Livermore National Laboratory, Livermore, California 94550, USA*
[2]*Princeton Plasma Physics Laboratory, Princeton, New Jersey 08540, USA*
[3]*General Atomics, San Diego, California 92186, USA*
[4]*University of California, Los Angeles, Los Angeles, California 90095, USA*
[5]*Massachusetts Institute of Technology, Cambridge, Massachusetts 02139, USA*

Experiments on the DIII-D tokamak have identified a novel regime in which applied resonant magnetic perturbations (RMPs) increase the particle confinement and overall performance. This Letter details a robust range of counter-current rotation over which RMPs cause this density pump-in effect for high confinement (H mode) plasmas. The pump in is shown to be caused by a reduction of the turbulent transport and to be correlated with a change in the sign of the induced neoclassical transport. This novel reversal of the RMP induced transport has the potential to significantly improve reactor relevant, three-dimensional magnetic confinement scenarios.

The tokamak, benefiting from good confinement due to toroidal symmetry [1], is the leading candidate device for the magnetic confinement of burning plasma for energy production. Tokamaks can never be fully axisymmetric, however, and always have some level of 3D fields whether due to intrinsic asymmetries in the device construction or purposefully applied. Small, core resonant error fields ($\delta B/B_0 \approx 10^{-4}$) can destroy confinement by locking magnetic islands and must be corrected with applied resonant magnetic perturbations (RMPs) [2–9]. In so doing, overall asymmetry is often amplified through the nonresonant spectrum of fields (the spectrum not inducing core islands). Reactor relevant high confinement (H mode, [10]) plasmas are subject to magnetohydrodynamic (MHD) instabilities called edge localized modes (ELMs) that are also mitigated or suppressed by purposefully breaking toroidal symmetry with RMPs [11–18]. Until now, it has been widely accepted that this breaking of the toroidal symmetry reduces particle confinement (referred to as "pump out"). A reduction of 15%–50% in confinement is common with the application of RMPs [12,13,16], due, in large part, to the formation of islands at the foot of the H-mode edge transport barrier or "pedestal" [19,20]. This level of density pump out is not necessary for core or edge stability, and much effort is being spent to minimize the degradation through complicated quasisymmetry optimizations [21] and real-time control techniques [22] in order to maximize fusion efficiency in the presence of RMPs. In contrast to these previous challenges, however, this report shows that RMPs naturally and robustly increase the particle confinement in certain rotation regimes of reactor relevant H-mode scenarios.

This Letter is unique in that it reports an observation of particle confinement improvement with the application of magnetic perturbations in H-mode plasmas. This is accompanied by a correspondingly novel reduction in edge turbulence with the application of RMPs. Past tokamak experiments have reported confinement improvements with applied nonaxisymmetric fields following from changes to the plasma-wall interactions [23] and stability of large transients [24]. Confinement has also been shown to improve due to a sign change in transport across non-axisymmetric magnetic islands in certain rotation conditions [25]. The transport changes reported in this Letter, however, are independent of increased wall interactions that are not sustainable in a reactor and not reliant on large dynamic instabilities in the plasma. Thus, the reported confinement improvement with RMPs is the first applicable to tokamak reactor scenarios. It also represents a novel physics regime in which axial asymmetry actually improves confinement over the axisymmetric case, which has important implications for all magnetically confined plasmas (stellarators, in particular).

In recent DIII-D experiments, the application of RMPs consistently caused the density to rise in ELMing H-mode discharges across a range of moderate counter-I_p rotations. I_p is the toroidal plasma current such that counter-I_p is the ion diamagnetic drift direction. The ELMs in these plasmas are associated with proximity to the kink-peeling stability boundary [26]. Experiments observing this phenomenon pulsed 3.4–5.7 kA, 310° $n = 2$ (n is the toroidal harmonic) perturbations using DIII-D's midplane error field correction ("C coil") array, which applies a mix of nonresonant and
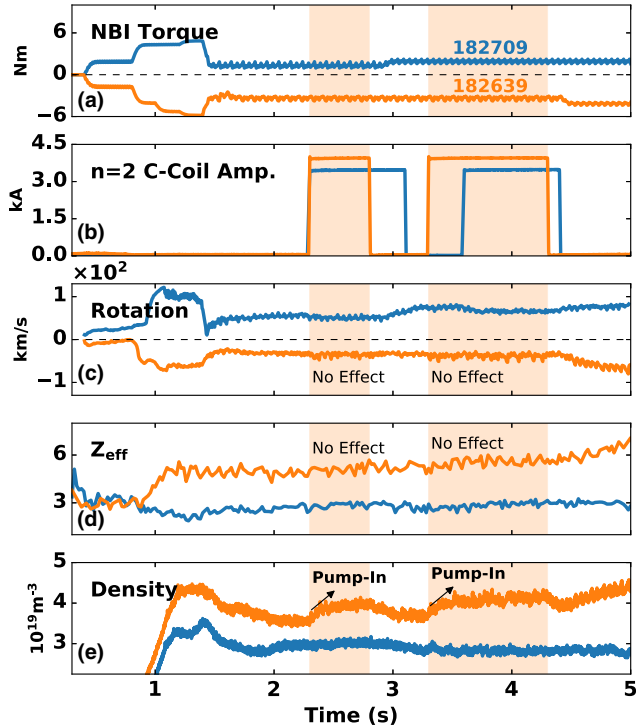
FIG. 1. With constant neutral beam injection torque (a), the application of $n = 2$ RMPs (b) in a discharge rotating (c) opposite I_p (orange) causes a sharp rise in electron density (d) without any correspondingly sudden change in plasma composition (c). The effect is not present in co-I_p rotation (blue).
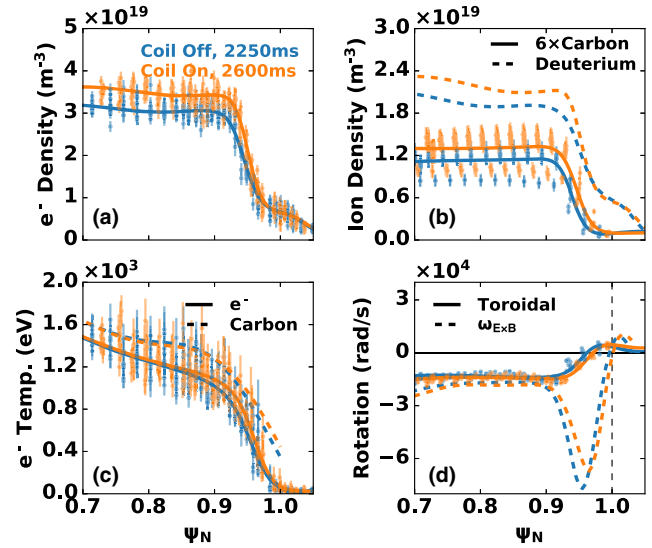

FIG. 2. Measured electron density (a), ion density (b), temperature (c), and rotation frequency (d) pedestal profiles before (blue) and after (orange) the application of RMPs in counter-I_p rotating shot 182 639. The densities rise while the temperatures and rotations are unaffected by the RMPs.

resonant magnetic perturbations [8,27]. The amplitude of this RMP is below any (as yet undiscovered) ELM suppression threshold that may exist in these scenarios and above the 1 kA I-coil equivalent $n = 2$ intrinsic error field [28]. The confinement improvement is immediately observable in the line integrated density measured by an interferometer channel directed through the core of the plasma, as shown in Fig. 1. Detailed profile analysis in Fig. 2 shows the RMPs raise the pedestal density with little change to the temperature or rotation. The figure shows Thomson scattering (electron) and charge exchange recombination spectroscopy (carbon impurity assumed to be equilibrated with the main plasma deuterium ion temperature) measurement data as well as lines indicating the radial basis function fits from OMFIT [29,30]. Quasineutrality has been assumed to calculate the main ion (deuterium) density and the profiles have been aligned to enforce the physical $\omega_{E \times B}(\psi_N = 1) = 0$ boundary constraint (the normalized poloidal flux ψ_N is 1 at the plasma separatrix). These detailed profiles confirm the pump in is, in fact, a confinement improvement impacting all species and not just an influx of impurities that increases the electron count.

The neutral beam injected torque was scanned between discharges, and Fig. 3(a) shows the increase in density when applying RMPs peaks at almost 6×10^{18} m^{-3},

amounting to a 15% increase in the density. The improvement is reduced at the most counter-I_p rotations obtained in this experiment, the furthest of which is complicated by being a quiescent H mode, [31,32]) with coherent edge MHD modes at counter-current pedestal rotations below -80 km/s. Here, the pedestal rotation is taken from charge exchange measurements at $\psi_N \approx 0.89$. No gas fueling feedback was used during these shots, and the line density (pedestal collisionality, ν_e^*) naturally varies from $2.6 - 4.3 \times 10^{19}$ m^{-3} (0.17–0.37) prior to RMP applications. These parameters do not separate the pump in and pump out, and relative change overlays in Fig. 3 show these variations do not impact the observed rotation dependence. Figure 3(b) shows that the density pump in corresponds to a rise in normalized pressure that peaks with an observation of 13% improvement, consistent with the rise in density at roughly constant temperature. Figure 3 also includes data from typical lower single null ELM control target plasmas reported in Ref. [28] (distinguished by ▼ markers) during the application of 4–4.6 kA $n = 2$ C-coil currents or 1.5 kA $n = 2$ currents in the internal I coils (shown in [28] to have comparable resonant coupling to 4.6 kA of C-coil current). This data shows the usual density pump out in positive rotations as well as hitherto unnoticed indications of pump in at the slightly negative rotations obtained.

The extensive suite of edge and plasma boundary diagnostics of DIII-D do not detect any changes in the wall particle source associated with the RMPs responsible for the observed rise in density. The exhaust rate, proportional to neutral pressure in the divertor region, is not impacted when the $n = 2$ RMP is applied. The Deuterium Balmer α (D_α) emissivity from tangential camera
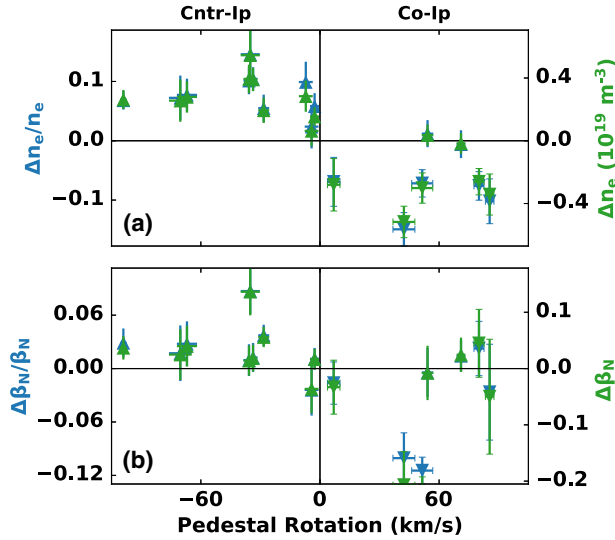
FIG. 3. The change in line integrated density (a) and normalized pressure (b). The observed improvements (blue) and fractional changes (green) behave similarly, peaking at moderate negative rotation and reversing when the rotation becomes positive with respect to the plasma current. Upper single null (shaded triangle) and lower single null (inverted shaded triangle) data is shown.

FIG. 4. ELM characteristics for counter-I_p rotating shot 182639 without (blue) and with (orange) RMPs. Black error bars show the mean and standard deviation of each dataset. The RMPs increases the size of the ELM density (a) and energy (b) crashes but increase the ELM period (c), resulting in no change to the average ELM particle flux (d). Thus, the observed pump-in (separation of on or off points in the horizontal axis) does not come from a change in ELM particle flux.

views [33] (proportional to the deuterium density) show no qualitative changes with the application of RMPs, indicating there is no change in particle sourcing. This is corroborated by the fact that Z_{eff} (the effective charge state of the plasma) does not change at these times. Thus, we conclude that the RMPs are modifying fundamental particle transport in the pedestal of these plasmas.

While no low-n MHD exists to be impacted in the ELMing H-mode plasmas, Fig. 4 shows that the ELMs become slightly larger with the application of the $n = 2$ RMP to these plasmas while their frequency decreases. The two effects effectively cancel when calculating the average ELM particle flux (the average rate at which ELM instabilities are expelling particles from the plasma). The difference in ELM fluxes with and without the RMP is $0.007 \pm 0.365 \times 10^{19}$ m^{-2} s^{-1}, with a value much smaller than the uncertainty. As the pump in exceeds the statistical variance in the density during the coil-free phases, this rules out changes in the ELM behavior as the cause of the pump in.

Note, the RMP pump in causes ELM changes that are opposite of the widely observed "ELM mitigation" phenomenon, wherein RMPs applied below the threshold for ELM suppression result in smaller and more frequent ELMs [34–36]. It is, however, consistent with the known dependencies of ELM size and frequency with density (horizontal axis) [37]. The rise in density results in the change of ELM size and frequency, not the other way around.

The observed change in particle confinement is also distinct from the resonant island physics proposed for ELM suppression [15,38] and particle pump out [39,40].
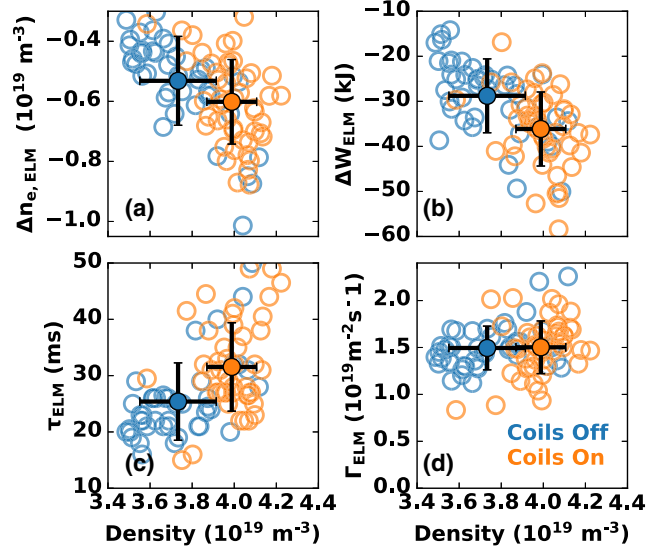
The pump-in plasmas have finite codirectional $E \times B$ and electron diamagnetic precession frequencies ($\omega_{E \times B}$ and ω_{*e}, respectively) throughout the pedestal, shielding islands and providing no inward resonant transport across rational surfaces (which would require $\omega_{E \times B}/\omega_{*e} < -1$ in resistive MHD [25]). The absence of islands, determined by nonlinear two-fluid MHD modeling using the TM1 code [39,40], means the transport mechanism responsible for the pump in does not need to overcome the common island induced pump out.

Generalized Perturbed Equilibrium Code (GPEC, [41,42]) calculations show the 3D-field-induced neoclassical non-ambipolar ion transport changes in the pedestal region are correlated with the observed changes in the particle confinement. Here, the pre-RMP profiles from Fig. 2 were used to form a kinetically constrained equilibrium from shot 182 639 and the measured toroidal rotation was artificially scaled within the GPEC model to calculate its impact on the neoclassical transport. GPEC is an equilibrium code and is not able to calculate the time dependent impact of this instantaneous flux. Simplified estimates of the modified density profiles using a constant effective diffusivity (D_{eff}) approximation, $n_{on} = -\int(\Gamma_{off} - \Gamma_{3D})/D_{eff} dr$, are shown in a black-red scale in Fig. 5(b). The axisymmetric flux Γ_{off} and effective diffusivity are calculated solving for power and particle balance using the ONETWO transport code [43] given the profiles from Fig. 2 prior to the RMP. The corresponding pedestal density change is shown in
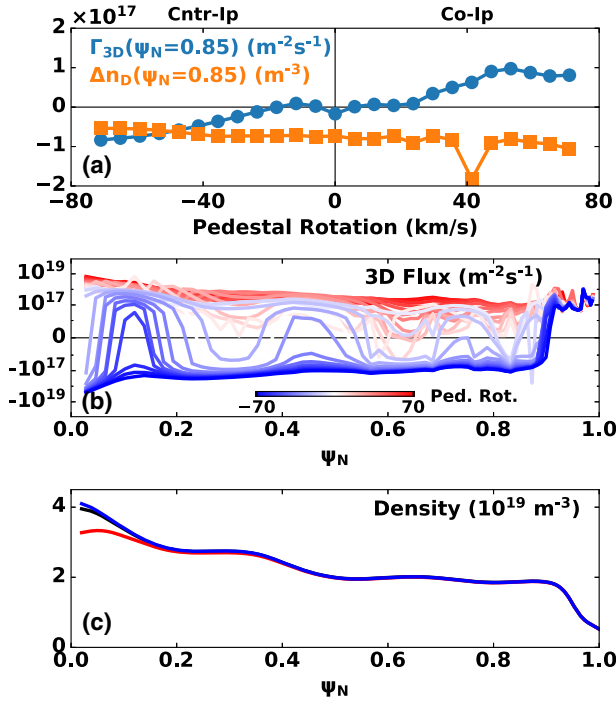
FIG. 5. Magnetic perturbation induced, neoclassical ion transport across flux surfaces. Axis (a) shows the flux at the pedestal top ($\psi_N = 0.85$) changes for negative rotations, but the linear estimate of pedestal density change does not. Axis (b) shows the neoclassical ion flux profiles, and (c) shows corresponding linear estimates of the extreme case density profiles, which are relatively small deviations from the original (black) profile.
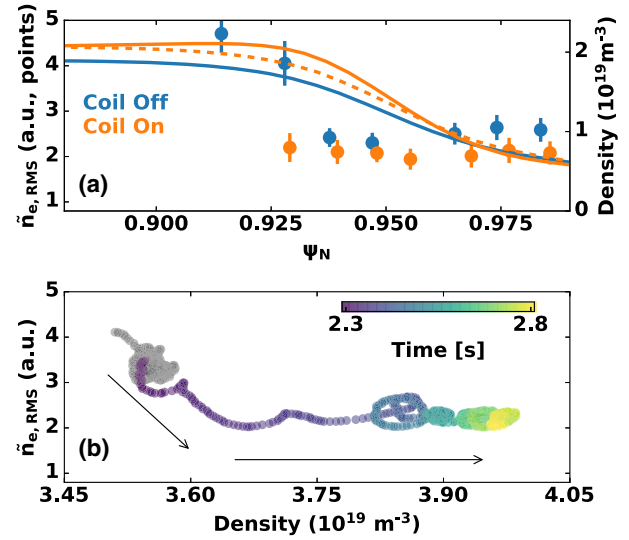

FIG. 6. DBS density fluctuation measurements in discharge 182 639. The fluctuations decrease across the entire pedestal when coils are applied (a), and have a causal influence on the observed density rise (b). The corresponding deuterium density model [(a), dashed line] is comparable to the experimental rise in the profiles [(a), solid lines].

Fig. 5(a) and is small (0.2%–1% change). It is always negative in this simple model because the edge $\omega_{E \times B}$, which is dominated by diamagnetic terms in the steep density gradient region, sets the sign of the midpedestal transport. Nonlinear studies have shown, however, that similar levels of the nonambipolar neoclassical transport that changes sign at the top of the pedestal here can couple to the primary transport mechanisms existent in the symmetric state and result in the experimentally observed levels of density change [44,45]. While the neoclassical model of torque reversals has been validated experimentally [46], this is the first observation of the particle transport reversing in a tokamak plasma and, thus, presents an opportunity for nonlinear modeling efforts to assess any possible contribution of this mechanism here.

The nonlinear interplay between the 3D induced transport and existing transport mechanisms is observed experimentally in the mitigation of turbulent fluctuations coincident with the applied fields. Doppler back scattering (DBS) [47] analysis for one of the peak pump-in pulses in Fig. 6(b) shows the density fluctuations with intermediate wave numbers ($k_\perp = 4\text{–}6$ cm^{-1} or $k_\perp \rho_s = 0.5\text{–}1.5$) changing quickly with the application of the fields. The density then rises on a transport time scale within this suppressed turbulence state. The fast decrease in fluctuations, followed by the slower rise in density establishes a causal relationship between the RMP induced turbulence changes and the pump in. A correspondingly sharp decrease in the measured phase velocity indicates that the decrease in the density fluctuation level is associated with a transition of the dominant inter-ELM turbulence from the ion mode to the electron mode at the pedestal top, while the steep gradient region remains dominated by ion-mode turbulence. Note, this decrease in turbulence is opposite previous observations of turbulence enhancement with RMPs [36,48,49], and the underlying reason the turbulent transport is reduced is not yet known.

The inter-ELM fluctuation profile measurements in Fig. 6(a) show that this turbulence reduction is a robust feature across the entire pedestal in these scenarios. Previous DIII-D measurements show that this enhanced inter-ELM edge turbulence measurement is highly correlated to increased particle transport [50]. A simple estimate of the ion density profile modification due to the change in turbulence is presented in Fig. 6(a) using the constant D_{eff} approximation. Here, the 3D-induced flux profile is approximated assuming linear dependence on the turbulence amplitude $\Gamma_{3D} = \Gamma_{\text{off}}(A_{\text{on}} - A_{\text{off}})/A_{\text{off}} \approx 0.3\text{–}1 \times 10^{19}$ m^{-2} s^{-1} in the outer radii where both amplitudes are available and assumed zero inside of this. Note, this is an order of magnitude larger than the modeled neoclassical particle flux and comparable to the $4 - 6 \times 10^{18}$ m^{-2} s^{-1} values of edge flux computed from the experimental profiles using $dn/dt = \nabla \cdot \Gamma_{3D}$ during the pump in. Accordingly, Fig. 6(a) shows the associated density change (calculated as in Fig. 5) corresponds to a

rise in the deuterium pedestal density comparable to the one experimentally observed. A direct measurement of cross-field flux (currently not possible on DIII-D due to a lack of perturbed velocity measurements), is highly desirable for future qualitative studies of this phenomenon. It is clear, however, that this is an important mechanism for the observed pump in.

In summary, DIII-D experiments have found a new regime in which RMPs like those planned for use in future H-mode reactors increase the particle confinement. A reduction in the turbulent particle transport with the application of RMPs is the dominant causal source of the pump in. The neoclassical particle transport induced when breaking the toroidal symmetry also changes sign at the top of the pedestal, and should be modeled in more detail to determine the full extent of it's role (if any) in the observed pump in. Both transport changes are distinct from the cross-island transport that causes pump out in L and H modes as well as any previously observed changed through sourcing or instabilities in L-mode plasmas. It is our hope that these new observations inspire 3D peeling mode model development to further understand the path to this stable rise in pedestal pressure. Future experimental work should test the relative diffusion and pinch transport terms in these regimes using gas puff modulation as well as test the compatibility between this confinement improvement and no ELM plasma regimes. While the pump-in regime does not have the $\omega_{E \times B}$ zero crossing thought to be required for ELM suppression in DIII-D, the improvements are uniquely compatible with the use of RMPs in a reactor to correct error fields or support ELM free scenarios such as quiescent H modes.

*logan35@llnl.gov
†Present address: Department of Applied Mathematics and Applied Physics, Columbia University, New York, New York 10027, USA.
‡Present address: General Atomics, San Diego, California 92186, USA.
§Present address: Princeton Plasma Physics Laboratory, Princeton, New Jersey 08540, USA.

[1] P. Helander, C. D. Beidler, T. M. Bird, M. Drevlak, Y. Feng, R. Hatzky, F. Jenko, R. Kleiber, J. H. Proll, Y. Turkin, and P. Xanthopoulos, Stellarator and tokamak plasmas: A comparison, Plasma Phys. Controlled Fusion **54**, 124009 (2012).

[2] R. Fitzpatrick and T. C. Hender, The interaction of resonant magnetic perturbations with rotating plasmas, Phys. Fluids B **3**, 644 (1991).

[3] R. J. La Haye, R. Fitzpatrick, T. C. Hender, A. W. Morris, J. T. Scoville, and T. N. Todd, Critical error fields for locked mode instability in tokamaks, Phys. Fluids B **4**, 2098 (1992).

[4] T. C. Hender, R. Fitzpatrick, A. W. Morris, P. G. Carolan, R. D. Durst, T. Edlington, J. Ferreira, S. J. Fielding, P. S. Haynes, J. Hugill, I. J. Jenkins, R. J. La Haye, B. J. Parham, D. C. Robinson, T. N. Todd, M. Valovic, and G. Vayakis, Effect of resonant magnetic perturbations on COMPASS-C tokamak discharges, Nucl. Fusion **32**, 2091 (1992).

[5] R. J. Buttery, M. De' Benedetti, D. A. Gates, Y. Gribov, T. C. Hender, R. J. La Haye, P. Leahy, J. A. Leuer, A. W. Morris, A. Santagiustina, J. T. Scoville, B. J. D. Tubbing (JET Team, COMPASS-D Research Team, and DIII-D Team), Error field mode studies on JET, COMPASS-D and DIII-D, and implications for ITER, Nucl. Fusion **39**, 1827 (1999).

[6] J.-K. Park, M. J. Schaffer, J. E. Menard, and A. H. Boozer, Control of Asymmetric Magnetic Perturbations in Tokamaks, Phys. Rev. Lett. **99**, 195003 (2007).

[7] J. E. Menard, R. E. Bell, D. A. Gates, S. P. Gerhardt, J.-K. Park, S. A. Sabbagh, J. W. Berkery, A. Egan, J. Kallman, S. M. Kaye, B. LeBlanc, Y. Q. Liu, A. Sontag, D. Swanson, H. Yuh, and W. Zhu, Progress in understanding error-field physics in NSTX spherical torus plasmas, Nucl. Fusion **50**, 045008 (2010).

[8] C. Paz-Soldan, M. J. Lanctot, N. C. Logan, D. Shiraki, R. J. Buttery, J. M. Hanson, R. J. La Haye, J.-K. Park, W. M. Solomon, and E. J. Strait, The importance of matched poloidal spectra to error field correction in DIII-D, Phys. Plasmas **21**, 072503 (2014).

[9] Y. In, J.-K. Park, Y. Jeon, J. Kim, G. Park, J.-W. Ahn, A. Loarte, W. Ko, H. Lee, J. Yoo, J. Juhn, S. Yoon, and H. Park, Enhanced understanding of non-axisymmetric intrinsic and controlled field impacts in tokamaks, Nucl. Fusion **57**, 116054 (2017).

[10] F. Wagner *et al.*, Regime of Improved Confinement and High Beta in Neutral-Beam-Heated Divertor Discharges of the ASDEX Tokamak, Phys. Rev. Lett. **49**, 1408 (1982).

[11] T. E. Evans *et al.*, Suppression of Large Edge-Localized Modes in High-Confinement DIII-D Plasmas with a Stochastic Magnetic Boundary, Phys. Rev. Lett. **92**, 235003 (2004).

[12] T. E. Evans, R. A. Moyer, K. H. Burrell, M. E. Fenstermacher, I. Joseph, A. W. Leonard, T. H. Osborne,

G. D. Porter, M. J. Schaffer, P. B. Snyder, P. R. Thomas, J. G. Watkins, and W. P. West, Edge stability and transport control with resonant magnetic perturbations in collisionless tokamak plasmas, Nat. Phys. **2**, 419 (2006).

[13] O. Schmitz *et al.*, Resonant Pedestal Pressure Reduction Induced by a Thermal Transport Enhancement due to Stochastic Magnetic Boundary Layers in High Temperature Plasmas, Phys. Rev. Lett. **103**, 165005 (2009).

[14] Y. M. Jeon, J.-K. Park, S. W. Yoon, W. H. Ko, S. G. Lee, K. D. Lee, G. S. Yun, Y. U. Nam, W. C. Kim, J.-G. Kwak, K. S. Lee, H. K. Kim, and H. L. Yang, Suppression of Edge Localized Modes in High-Confinement KSTAR Plasmas by Nonaxisymmetric Magnetic Perturbations, Phys. Rev. Lett. **109**, 035004 (2012).

[15] R. Nazikian *et al.*, Pedestal Bifurcation and Resonant Field Penetration at the Threshold of Edge-Localized Mode Suppression in the DIII-D Tokamak, Phys. Rev. Lett. **114**, 105002 (2015).

[16] C. Paz-Soldan, R. Nazikian, S. R. Haskey, N. C. Logan, E. J. Strait, N. M. Ferraro, J. M. Hanson, J. D. King, M. J. Lanctot, R. A. Moyer, M. Okabayashi, J.-K. Park, M. W. Shafer, and B. J. Tobias, Observation of a Multimode Plasma Response and its Relationship to Density Pumpout and Edge-Localized Mode Suppression, Phys. Rev. Lett. **114**, 105001 (2015).

[17] Y. Sun *et al.*, Nonlinear Transition from Mitigation to Suppression of the Edge Localized Mode with Resonant Magnetic Perturbations in the EAST Tokamak, Phys. Rev. Lett. **117**, 115001 (2016).

[18] J.-K. Park, Y. Jeon, Y. In, J.-W. Ahn, R. Nazikian, G. Park, J. Kim, H. Lee, W. Ko, H.-S. Kim, N. C. Logan, Z. Wang, E. A. Feibush, J. E. Menard, and M. C. Zarnstorff, 3D field phase-space control in tokamak plasmas, Nat. Phys. **14**, 1223 (2018).

[19] Q. M. Hu, R. Nazikian, N. C. Logan, J.-K. Park, C. Paz-Soldan, S. M. Yang, B. A. Grierson, Y. In, Y. M. Jeon, M. Kim, S. K. Kim, D. M. Orlov, G. Y. Park, and Q. Yu, Predicting operational windows of ELMs suppression by resonant magnetic perturbations in the DIII-D and KSTAR tokamaks, Phys. Plasmas **28**, 052505 (2021).

[20] Q. Hu, J.-K. Park, N. Logan, S. Yang, B. Grierson, R. Nazikian, and Q. Yu, Nonlinear two-fluid modeling of plasma response to RMPs for the ELM control in the ITER baseline, Nucl. Fusion **61**, 106006 (2021).

[21] J.-K. Park, S. M. Yang, N. C. Logan, Q. Hu, C. Zhu, M. C. Zarnstorff, R. Nazikian, C. Paz-Soldan, Y. M. Jeon, and W. H. Ko, Quasisymmetric Optimization of Nonaxisymmetry in Tokamaks, Phys. Rev. Lett. **126**, 125001 (2021).

[22] S. Kim, R. Shousha, S. Hahn, A. Nelson, J. Wai, S. Yang, J.-K. Park, R. Nazikian, N. Logan, Y. Jeon, Y. In, J. Lee, J. Kim, C. Lee, Y.-S. Na, and E. Kolemen, Optimization of 3D controlled ELM-free state with recovered global confinement for KSTAR with $n = 1$ resonant magnetic field perturbation, Nucl. Fusion **62**, 026043 (2022).

[23] K. H. Finken, S. S. Abdullaev, M. W. Jakubowski, M. F. M. de Bock, S. Bozhenkov, C. Busch, M. von Hellermann, R. Jaspers, Y. Kikuchi, A. Krämer-Flecken, M. Lehnen, D. Schega, O. Schmitz, K. H. Spatschek, B. Unterberg, A. Wingen, R. C. Wolf, and O. Zimmermann, Improved Confinement due to Open Ergodic Field Lines Imposed

by the Dynamic Ergodic Divertor in TEXTOR, Phys. Rev. Lett. **98**, 065001 (2007).

[24] T. Evans, M. Goniche, A. Grosman, D. Guilhem, W. Hess, and J.-C. Vallet, Magnetic perturbation effects on boundary plasmas during high power lower hybrid current drive in Tore Supra, J. Nucl. Mater. **196–198**, 421 (1992).

[25] Q. Hu, Q. Yu, N. Wang, P. Shi, B. Yi, Y. Ding, B. Rao, Z. Chen, L. Gao, X. Hu, H. Jin, M. Li, J. Li, K. Yu, G. Zhuang, and J.-T. Team, Influence of rotating resonant magnetic perturbations on particle confinement, Nucl. Fusion **54**, 122006 (2014).

[26] P. B. Snyder, H. R. Wilson, J. R. Ferron, L. L. Lao, A. W. Leonard, T. H. Osborne, A. D. Turnbull, D. Mossessian, M. Murakami, and X. Q. Xu, Edge localized modes and the pedestal: A model based on coupled peeling-ballooning modes, Phys. Plasmas **9**, 2037 (2002).

[27] R. J. La Haye, S. Gunter, D. A. Humphreys, J. Lohr, T. C. Luce, M. E. Maraschek, C. C. Petty, R. Prater, J. T. Scoville, and E. J. Strait, Control of neoclassical tearing modes in DIII-D, Phys. Plasmas **9**, 2051 (2002).

[28] C. Paz-Soldan, N. Logan, M. Lanctot, J. Hanson, J. King, R. La Haye, R. Nazikian, J.-K. Park, and E. Strait, Decoupled recovery of energy and momentum with correction of $n = 2$ error fields, Nucl. Fusion **55**, 083012 (2015).

[29] O. Meneghini *et al.*, Integrated modeling applications for tokamak experiments with OMFIT, Nucl. Fusion **55**, 083008 (2015).

[30] N. Logan, B. Grierson, S. Haskey, S. Smith, O. Meneghini, and D. Eldon, OMFIT tokamak profile data fitting and physics analysis, Fusion Sci. Technol. **74**, 125 (2018).

[31] C. M. Greenfield, K. H. Burrell, J. C. Deboo, E. J. Doyle, B. W. Stallard, E. J. Synakowski, C. Fenzi, P. Gohil, R. J. Groebner, L. L. Lao, M. A. Makowski, G. R. Mckee, R. A. Moyer, C. L. Rettig, T. L. Rhodes, R. I. Pinsker, G. M. Staebler, W. P. West, and D.-D. Team, Quiescent Double Barrier Regime in the DIII-D Tokamak, Phys. Rev. Lett. **86**, 4544 (2001).

[32] K. H. Burrell, A. M. Garofalo, W. M. Solomon, M. E. Fenstermacher, T. H. Osborne, J.-K. Park, M. J. Schaffer, and P. B. Snyder, Reactor-relevant quiescent H-mode operation using torque from non-axisymmetric, non-resonant magnetic fields, Phys. Plasmas **19**, 056117 (2012).

[33] C. J. Lasnier, S. L. Allen, R. E. Ellis, M. E. Fenstermacher, A. G. McLean, W. H. Meyer, K. Morris, L. G. Seppala, K. Crabtree, and M. A. V. Zeeland, Wide-angle ITER-prototype tangential infrared and visible viewing system for DIII-Da), Rev. Sci. Instrum. **85**, 11D855 (2014).

[34] I. T. Chapman, A. Kirk, S. Saarelma, J. R. Harrison, and R. Scannell, Towards understanding ELM mitigation: The effect of axisymmetric lobe structures near the X-point on ELM stability, Nucl. Fusion **52**, 123006 (2012).

[35] A. Kirk, I. T. Chapman, Y. Liu, P. Cahyna, P. Denner, G. Fishpool, C. J. Ham, J. R. Harrison, Y. Liang, E. Nardon, S. Saarelma, R. Scannell, and A. J. Thornton, Understanding edge-localized mode mitigation by resonant magnetic perturbations on MAST, Nucl. Fusion **53**, 043007 (2013).

[36] F. Zhong, T. Zhang, Y. Wang, F. Wen, J. Huang, M. Wu, G. Li, Y. Liu, K. Geng, H. Xiang, K. Ye, Z. Zhou, X. Han, L. Meng, L. Wang, Y. Sun, and X. Gao, Observation of enhanced pedestal turbulence during ELM mitigation with

resonant magnetic perturbation on EAST, AIP Adv. **11,** 075010 (2021).

[37] A. Loarte, G. Saibene, R. Sartori, D. Campbell, M. Becoulet, L. Horton, T. Eich, A. Herrmann, G. Matthews, N. Asakura, A. Chankin, A. Leonard, G. Porter, G. Federici, G. Janeschitz, M. Shimada, and M. Sugihara, Characteristics of type I ELM energy and particle losses in existing devices and their extrapolation to ITER, Plasma Phys. Controlled Fusion **45,** 1549 (2003).

[38] Q. Hu, N. C. Logan, J.-K. Park, C. Paz-Soldan, R. Nazikian, and Q. Yu, Nonlinear modeling of the scaling law for the $m/n = 3/2$ error field penetration threshold, Nucl. Fusion **60,** 076006 (2020).

[39] Q. Hu, R. Nazikian, B. Grierson, N. Logan, C. Paz-Soldan, and Q. Yu, The role of edge resonant magnetic perturbations in edge-localized-mode suppression and density pump-out in low-collisionality DIII-D plasmas, Nucl. Fusion **60,** 076001 (2020).

[40] Q. M. Hu, R. Nazikian, B. A. Grierson, N. C. Logan, J.-K. Park, C. Paz-Soldan, and Q. Yu, The density dependence of edge-localized-mode suppression and pump-out by resonant magnetic perturbations in the DIII-D tokamak, Phys. Plasmas **26,** 120702 (2019).

[41] J.-K. Park and N. Logan, Self-consistent perturbed equilibrium with neoclassical toroidal torque in tokamaks, Phys. Plasmas **24,** 032505 (2017).

[42] N. C. Logan, J.-K. Park, K. Kim, Z. Wang, and J. W. Berkery, Neoclassical toroidal viscosity in perturbed equilibria with general tokamak geometry, Phys. Plasmas **20,** 122507 (2013).

[43] H. St. John, T. Taylor, Y. Lin-Liu, and A. Turnbull, Transport simulation of negative magnetic shear discharges, Plasma Phys. Controlled Nucl. Fusion Res. **3,** 603 (1994).

[44] Y. Liu, C. Paz-Soldan, L. Li, and Y. Sun, Role of 3-D neoclassical particle flux in density pump-out during ELM control by RMP in DIII-D, Nucl. Fusion **60,** 036018 (2020).

[45] S. K. Kim, S. Pamela, N. C. Logan, Y.-S. Na, J.-K. Park, S. M. Yang, M. Becoulet, M. Hoelzl, G. Huijsmans, Q. Hu, Y. In, M. W. Kim, O. Kwon, C. Y. Lee, H. H. Lee, J. Lee, J. H. Lee, E. Kolemen, and J. Team, Nonlinear MHD modeling of $n = 1$ RMP-induced pedestal transport and mode coupling effects on ELM suppression in KSTAR, Nucl. Fusion **62,** 106021 (2022).

[46] A. M. Garofalo, K. H. Burrell, J. C. DeBoo, J. S. deGrassie, G. L. Jackson, M. Lanctot, H. Reimerdes, M. J. Schaffer, W. M. Solomon, and E. J. Strait, Observation of Plasma Rotation Driven by Static Nonaxisymmetric Magnetic Fields in a Tokamak, Phys. Rev. Lett. **101,** 195005 (2008).

[47] W. A. Peebles, T. L. Rhodes, J. C. Hillesheim, L. Zeng, and C. Wannberg, A novel, multichannel, comb-frequency Doppler backscatter system, Rev. Sci. Instrum. **81,** 10D902 (2010).

[48] G. R. McKee, Z. Yan, C. Holland, R. J. Buttery, T. E. Evans, R. A. Moyer, S. Mordijck, R. Nazikian, T. L. Rhodes, O. Schmitz, and M. R. Wade, Increase of turbulence and transport with resonant magnetic perturbations in ELM-suppressed plasmas on DIII-D, Nucl. Fusion **53,** 113011 (2013).

[49] J. Lee, G. S. Yun, M. J. Choi, J. M. Kwon, Y. M. Jeon, W. Lee, N. C. Luhmann, and H. K. Park, Nonlinear Interaction of Edge-Localized Modes and Turbulent Eddies in Toroidal Plasma under $n = 1$ Magnetic Perturbation, Phys. Rev. Lett. **117,** 075001 (2016).

[50] R. Hong, T. L. Rhodes, Z.-Y. Li, H. Wang, L. Zeng, K. Barada, G. Wang, J. G. Watkins, and W. A. Peebles, Observation of quasi-coherent density fluctuation in scrape-off layer enhancing boundary transport in high-βN hybrid plasmas on DIII-D, Plasma Phys. Controlled Fusion **63,** 065015 (2021).